Antibacterial Layer-by-Layer Films of Poly(acrylic acid)–Gentamicin Complexes with a Combined Burst and Sustainable Release of Gentamicin

*Ane Escobar, Nicolás E. Muzzio, Patrizia Andreozzi, Sara Libertone, Elisamaria Tasca, Omar Azzaroni, Marek Grzelczak, and Sergio E. Moya**

There is an urgent need for the development of effective antibacterial coatings to cope with more and more resistant bacterial strains in medical environments, and particularly to prevent nosocomial infections following bone implant surgery. Polyelectrolyte multilayers (PEMs) based on poly-L-lysine (PLL) and complexes of poly(acrylic acid) (PAA) and gentamicin have been fabricated here applying the layer-by-layer (LbL) technique. Complexes are prepared by mixing PAA and gentamicin solutions in 500×10^{-3} M NaCl at pH 4.5. The assembly of PLL and the complexes follows an exponential growth allowing a high loading of gentamicin in a four bilayer PEM. Although PEMs are stable and do not degrade at physiological pH, there is a continuous release of gentamicin at pH 7.4. PEMs show an initial burst release of gentamicin in the first 6 h, which liberates 58% of the total gentamicin released during the experiment, followed by a sustainable release lasting over weeks. This release profile makes the coating appealing for the surface modification of bone implants as a high concentration of antibiotics is necessary during implant surgery while a lower antibiotic concentration is needed until tissue is regenerated. PEMs are effective in preventing the proliferation of the *Staphylococcus aureus* strain.

1. Introduction

The widespread nature of bacterial infections and their increasing resistance to antibiotics has led to the development of antibacterial coatings in multiple medical settings, especially on bone implants.[1] The surface of implants is susceptible to numerous bacterial infections mainly because of the formation of a surface biofilm and the compromised immune response at the implant/tissue interface. *Staphylococcus aureus* and *Staphylococcus epidermidis* are among the most common strains that cause implant associated infections.[2] *S. aureus* is considered a major virulent pathogen that colonizes and infects both hospitalized patients with decreased immunity and healthy immunocompetent people. Although this bacterium is found naturally on the skin and in the nasopharynx of the human body, the environment within a hospital supports the acquisition of resistant *S. aureus* strains. Skin and mucous membranes are excellent barriers against local tissue invasion by *S. aureus*. However, if these barriers are breached due to trauma or surgery, *S. aureus* can enter the underlying tissue, creating local abscess lesion, and may further progress to the lymphatic channels or blood, where it can cause septicemia.[3,4] Once a biofilm is formed, it protects adherent bacteria from the host defense system and bactericidal agents via several mechanisms.[5–7] The biofilm becomes a source of pathogens and infections, being the cause of so called nosocomial infections, infections acquired in a hospital or healthcare unit.[8–10] Nosocomial infections are secondary to the main condition of the patient, and can have lethal consequences following operations such as bone replacement or open heart surgery.[11–13] Because biofilms can form on almost any material present in a surgery room, prevention of their formation can be fundamental for patient survival. Unfortunately, there are still no good means to eliminate the infection developed through an implant surgery. Currently, implant removal is the only strategy to eradicate the infections and the immune response of the host to the implant is consequently impaired. In the early phase after implantation, the local defense system is severely disturbed by the surgical trauma. Thus, prevention

Dr. A. Escobar, Dr. N. E. Muzzio, Dr. P. Andreozzi, S. Libertone,
Dr. S. E. Moya
CIC biomaGUNE
Paseo de Miramón 182, 20014 Donostia-San Sebastián, Spain
E-mail: smoya@cicbiomagune.es
E. Tasca
Department of Chemistry
University "La Sapienza"
Ple. Aldo Moro 5, 00185 Rome, Italy
Dr. O. Azzaroni
Instituto de Investigaciones Fisicoquímicas Teóricas y Aplicadas
(INIFTA)
(UNLP, CONICET)
Sucursal 4, Casilla de Correo 16, 1900 La Plata, Argentina
Dr. M. Grzelczak
Ikerbasque
Basque Foundation for Science
48013, Bilbao, Spain
Dr. M. Grzelczak
Donostia International Physics Center
Paseo de Manuel Lardizabal 4, 20018 Donostia-San Sebastián, Spain

The ORCID identification number(s) for the author(s) of this article can be found under https://doi.org/10.1002/admi.201901373.

DOI: 10.1002/admi.201901373

**ADVANCED
SCIENCE NEWS**
www.advancedsciencenews.com

**ADVANCED
MATERIALS
INTERFACES**
www.advmatinterfaces.de

of the initial stage of pathogenesis around implants is critical to ensure the success of implant surgery.[14,15]

Several strategies have been proposed to develop antibacterial coatings. A simple approach involves the functionalization of materials with cationic polymers that disrupt bacterial membranes causing their death.[1,16–18] The encapsulation of antibiotics in polymer matrixes is an attractive approach for the fabrication of antibacterial coatings. These coatings are usually made out of hydrogels, layer-by-layer (LbL) assemblies, polymer brushes or porous polymer scaffolds.[16–25] A major drawback of the encapsulation of antibiotics in polymer films is the difficulty in achieving a slow release of antibiotics. In addition, often the coating degrades accompanied by liberation of the antibiotics all at once, or at a rate faster than required. An optimal antibacterial coating for bone implants based on antibiotic release should combine an initial burst release at the time of surgery followed by prolonged release over the weeks following the chirurgical intervention to ensure bone tissue regeneration.[1,26]

The LbL technique involves the alternating assembly of oppositely charged polyelectrolytes through electrostatic interactions, offering multiple possibilities for the noncovalent modification of any surface for device fabrication. The LbL technique has been used for the engineering of scaffolds and implants to assemble growth factors and other molecules that facilitate tissue regeneration or enhance cell adhesion.[27–33] Polyelectrolyte multilayers (PEMs) assembled by the LbL technique display either a linear or exponential growth.[34,35] In a linear growth, the amount of assembled polyelectrolyte is linearly proportional to the number of deposited layers, while in an exponential or supralineal regime the amount of polyelectrolyte per layer increases as the number of assembled layers increase in a nonlinear dependence. The occurrence of a lineal or an exponential growth depends on the characteristics of the polyelectrolyte building blocks. Other materials such as nanoparticles, lipids, proteins, or clays have also been assembled in the LbL fashion.[36–39] Molecular complexes, stable colloidal aggregates of molecules bound by week interactions, have also been employed as building blocks for the fabrication of PEMs. For example, G. Romero et al.[40] have shown that complexes of alginate and the antiTNF-α antibody can be assembled in LbL, while the direct assembly of the antibody does not result in stable layers because of the weak charge of antiTNF-α.

Recently, Moskowitz et al.[8] proposed an antibacterial coating with an initial burst release of gentamicin followed by slow release. The coating was formed by a tetralayer unit containing gentamicin sulphate, poly(acrylic acid) (PAA) and a synthetic poly(β-amino ester) (Poly 1), combined as PAA/Poly 1/PAA/Gentamicin. Gentamicin is a frequently used antibiotic, an aminoglycan displaying three primary amine groups, which can interact with PAA through electrostatic interactions and hydrogen bonding. The entire film comprised 200 tetralayers, achieved over 5 d using an automated fabrication method.[8]

In this work we propose a simple method for the fabrication of antibacterial coatings employing the LbL technique. Using PAA–gentamicin complexes as building blocks with poly-L-lysine (PLL), we create a coating in just a few assembly steps with enough gentamicin loading to exhibit antibacterial properties. The PAA–gentamicin complexes act in the

multilayer as reservoir for gentamicin, which is liberated first in a burst release and then slowly over weeks at physiological pH. The interaction of PAA with PLL results in a stable film despite the release of gentamicin. The novel supramolecular architecture presented here is particularly appealing for the development of antibacterial coatings to prevent acquisition of nosocomial infections in various medical settings.

2. PAA–Gentamicin Complexes

PAA–gentamicin complexes were prepared by mixing PAA and gentamicin solutions (**Figure 1**A) at different gentamicin and NaCl concentrations at pH 4.5. At this pH the amines of gentamicin are largely protonated and positively charged since the pKa for gentamicin is in the range of 5.5 and 9. It can also be expected that carboxylate groups from PAA are to a large extent deprotonated and negatively charged as the pKa for PAA is 3.9.[41,42] Therefore, we decided to work at pH 4.5, which is an intermediate value between the pKa of PAA and the pKa of gentamicin, and ensures that the two molecules are oppositely charged and with enough charge to form stable complexes. Salt concentration is tuned to obtain the most stable complexes with the highest gentamicin concentration. As observed by dynamic light scattering (DLS) (Figure S1, Supporting Information), without salt (Figure S1a, Supporting Information) or with 10×10^{-3} M NaCl (Figure S1b, Supporting Information), complexes start to form with 0.1 mg mL^{-1} of gentamicin, but they do not show a stable size when the concentration of gentamicin is 0.25 mg mL^{-1} or higher. In both cases the size of the complexes increases by more than 100% after 4 h. The increase in size of the complexes implies also that the number of complexes in bulk will diminish. In water, for 0.45 mg mL^{-1} gentamicin, complexes start to precipitate after 4 h. However, DLS also shows smaller complexes present in solution that do not precipitate. At 500×10^{-3} M NaCl, complexes start to form with at least 0.3 mg mL^{-1} of gentamicin, but if the concentration of gentamicin is increased to 0.45 mg mL^{-1} the size of the complexes is not stable, changing with time (Figure S1c, Supporting Information). After 4 h the size of the complexes is three times larger than their size measured immediately after preparation. At high salt concentration (2 M) the formation of complexes is suppressed (Figure S1d, Supporting Information). FTIR of the complexes, Figure S2 (Supporting Information), reveals the presence of characteristic bands of PAA and gentamicin in the complexes. However, the formation of the complexes induces a slight shift in the N–H stretching band from gentamicin from 3590 to around 3570 cm^{-1}. In parallel, the O–H stretching band of carboxylates of PAA moves from 3380 to 3370 cm^{-1}. Both bands largely superpose but their shift can be clearly distinguished. Also, the carbonyl band at 1670 cm^{-1} and the N–H at 1690 cm^{-1} largely superpose in the complexes and shift to 1650 cm^{-1}. The shifts of the C–OH, carbonyl, and N–H bands are indicative of the complexation of the carboxylates from PAA and the amines of gentamicin.[43] The electrostatic interactions and hydrogen bond between amines and carboxylates should influence the stretching modes of the bounds from both amines and carboxylates and in the energy associated. No shift in the C–H band at 1530 cm^{-1} is observed

**ADVANCED
SCIENCE NEWS**

www.advancedsciencenews.com

**ADVANCED
MATERIALS
INTERFACES**

www.advmatinterfaces.de
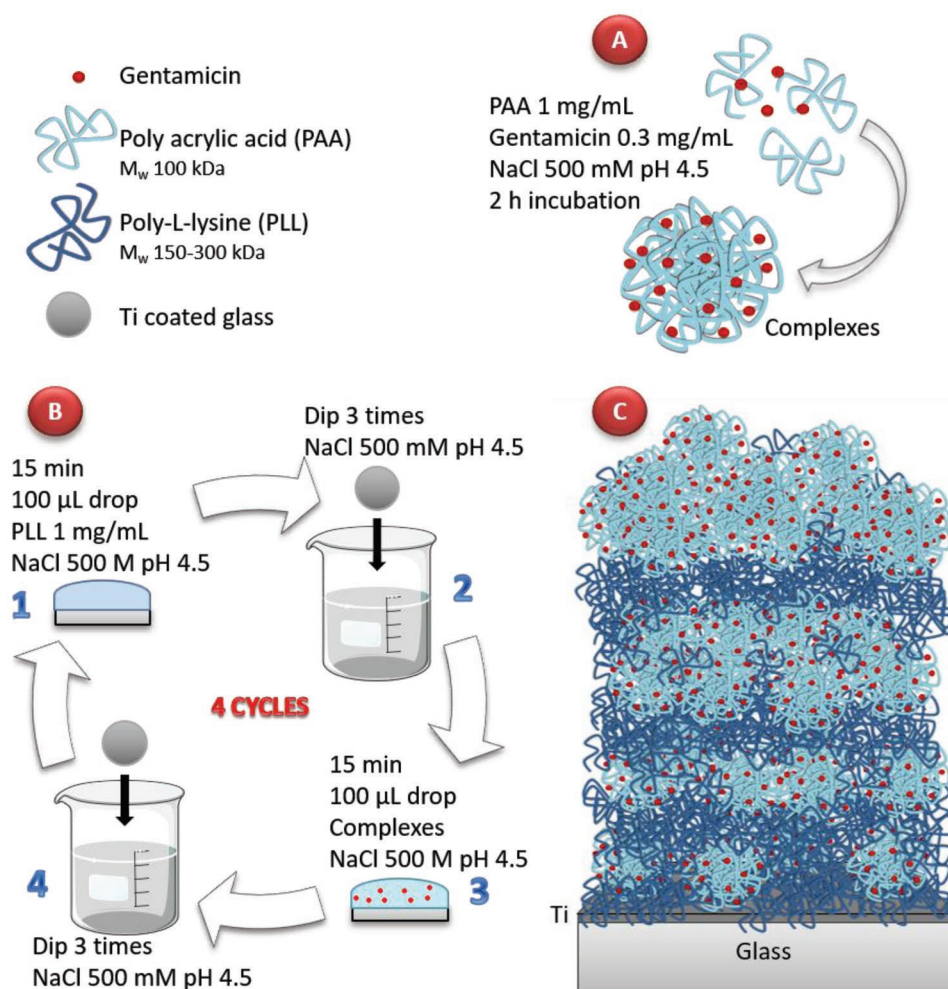
Figure 1. A) Scheme of the formation of gentamicin and PAA complexes in 500×10^{-3} M NaCl at pH 4.5. B) LbL assembly of PLL and PAA–gentamicin complexes. The LbL assembly was performed in 500×10^{-3} M NaCl at pH 4.5 in four steps: (1) 15 min incubation of 100 µL drop of 1 mg mL^{-1} PLL, (2) removal of the PLL that has not been adsorbed by dipping the substrate in 500×10^{-3} M NaCl pH 4.5, (3) 15 min incubation of 100 µL drop of PAA–gentamicin complexes, and (4) removal of the complexes that have not been adsorbed by dipping the substrate in 500×10^{-3} M NaCl pH 4.5. This cycle is repeated four times. (C) Scheme of PEMs showing four bilayers of PLL/PAA–gentamicin complexes grown on top of titania films.

in the complexes as this not affected by the interaction between amines and carboxylates.

Antibacterial activity of the coating can be enhanced with a high gentamicin content but increasing gentamicin concentrations lead to larger and more unstable complex sizes. 0.3 mg mL^{-1} is the largest gentamicin concentration that leads

to complexes with relatively stable size within the 2 h that the layer-by-layer assembly lasts. We monitored the evolution of the hydrodynamic diameter of the complexes over time using constant gentamicin concentration (0.3 mg mL^{1}) and varying salt concentration (0–2 M) (**Table 1**). At high salt concentrations (2 M), the formation of complexes is suppressed. The resulting

Table 1. Time evolution of the hydrodynamic diameter of PAA–gentamicin complexes prepared with 0.3 mg mL^{-1} gentamicin and different NaCl concentrations at pH 4.5. DLS measurements of complexes were conducted immediately after preparation, and 2 and 4 h after complex preparation. Complexes were prepared with 0.3 mg mL^{-1} of gentamicin in water and 10×10^{-3} M, 500×10^{-3} M, and 2 M NaCl. The standard deviation calculated from three replicates is shown.

Ionic Strength	Hydrodynamic diameter (± SD)		
	0 h	2 h	4 h
H$_2$O	382.1 ± 80.8 nm	774 ± 147 nm	831.6 ± 143.6 nm
NaCl 10×10^{-3} m	596.3 ± 102.6 nm	1121 ± 171.1 nm	1570 ± 229.3 nm
NaCl 500×10^{-3} m	177.7 ± 48.7 nm	276.3 ± 72.5 nm	293 ± 59.3 nm
NaCl 2 M	29.67 ± 5.8 nm	30.13 ± 8.8 nm	33.74 ± 11.5 nm

hydrodynamic diameter of ≈30 nm corresponds to free PAA of 100 kDa under the same NaCl and pH conditions. At low salt concentration (10×10^{-3} M), the size of the complexes is relatively large, >1500 nm, leading to their precipitation after 4 h. We found that at 500×10^{-3} M of NaCl the complexes maintained their size invariable (120–300 nm), during the first 4 h after formation. More detailed analysis of size distributions from DLS revealed the presence of two peaks of 25 and 180 nm, just after mixing both components (**Figure 2**a). After 2 h the smallest peak disappears while the second peak shifts to higher values and is narrower, meaning that the larger complexes increase their size at the expense of the smaller ones, most likely decreasing in number as well. At 4 h, the peak is slightly shifted to higher sizes and seems to continue to narrow, but we consider that the size distribution has practically not changed from 2 to 4 h after assembly of the complexes. Differently from DLS analysis, transmission electron microscopy (TEM) characterization of the sample two hours after mixing gentamicin and PAA shows the presence of small and large complexes ranging from 60 to 350 nm in diameter (Figure 2b), suggesting that the scattering intensity of the small complexes at 2 h is shielded by the much larger scattering of the large complexes. For further experiments we selected the complexes that were prepared with 0.3 mg mL^{-1} gentamicin and 500×10^{-3} M of NaCl.

A cell viability study was conducted with MC3T3-E1 cells in presence of PAA–gentamicin complexes. MTT assay shows no effect on cell proliferation, hinting no toxicity for the complexes (Figure S3, Supporting Information).

3. Layer-by-Layer Assembly of PLL/PAA–Gentamicin Complexes

PAA–gentamicin complexes display a ζ-potential of −12,6 ± 2,7 mV, which allows their assembly in LbL films. PLL and PAA–gentamicin complexes were alternately deposited on titania films, as depicted in Figure 1B. The assembly of the four bilayers of PLL and PAA–gentamicin complexes was monitored by the Quartz Crystal Microbalance with dissipation technique (QCM-D) (**Figure 3**a). With the increase of a material on top of QCM-D sensor the frequency shifts to lower values.[44,45] The deposition of each layer of PLL and complexes causes the decrease frequency. PLL layers show the following frequency values: 8, 11, 51, 73 Hz from the

first to the four layer respectively. PAA–gentamicin layers show larger frequency shifts: 34, 57, 85, and 191 Hz, from the first to the four layer deposited respectively. Frequency changes suggest that the LbL assembly follows an exponential growth (Figure 3b).[34,46–48] The exponential growth implies an increase
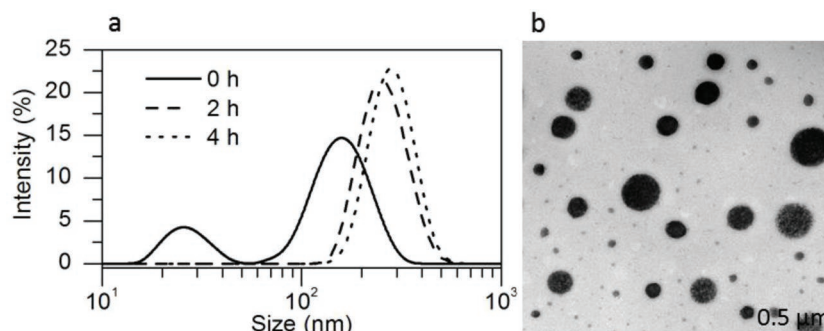
Figure 2. a) Intensity plot of size distribution at different times after complex formation for PAA–gentamicin complexes prepared in 500×10^{-3} M NaCl at pH 4.5 with 0.3 mg mL^{-1} gentamicin. b) TEM image of complexes 2 h after preparation.
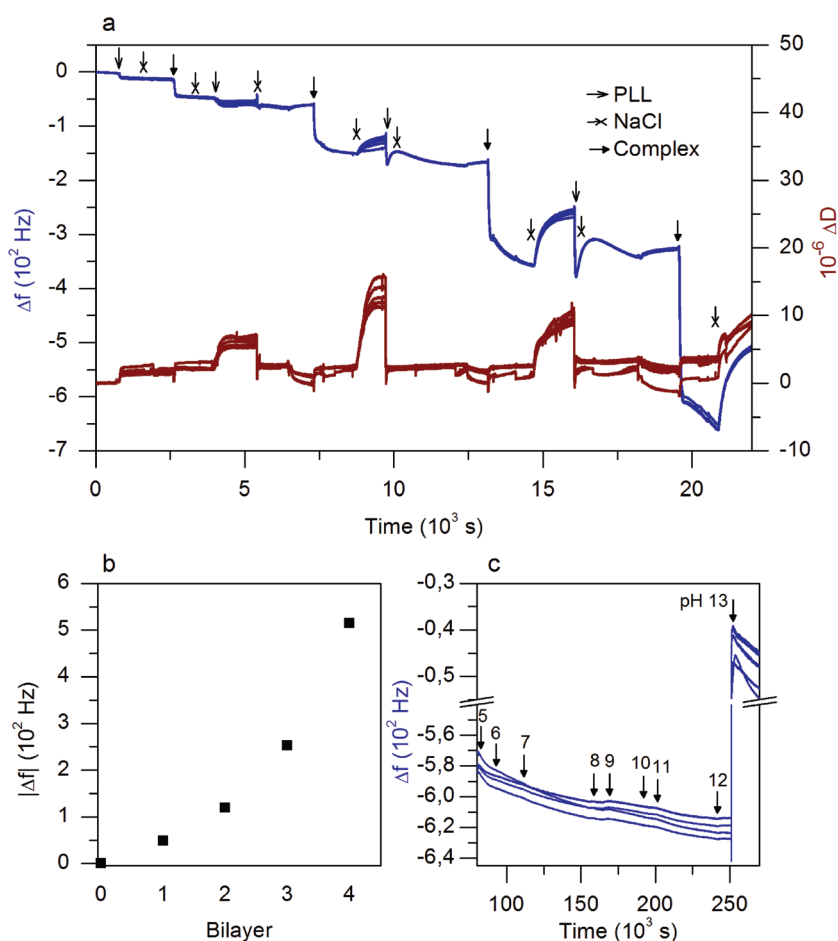
Figure 3. QCM-D monitoring of layer-by-layer assembly of PLL and PAA–gentamicin complexes prepared with 0.3 mg mL^{-1} gentamicin and film degradation. a) Frequency and dissipation variations during the LbL assembly of four bilayers of PLL and PAA–gentamicin (0.3 mg mL^{-1}) complexes in 500×10^{-3} M NaCl and pH 4.5, b) plot of frequency changes after each bilayer is deposited, and c) Changes in frequency in 500×10^{-3} M NaCl increasing the pH from 5 to 13.

in the amount of PLL and PAA–gentamicin complexes per layer as the number of assembled layers increases. Since complexes can be considered as spherical nanoparticle of ≈100 nm the deposition of each layer results in an increase in the area available for assembly of the next PLL layer. The increase in available free area allows for the deposition of more PLL than on a planar surface. This situation repeats as the assembly proceeds. Consequently, the top layer will contain more complexes and more gentamicin than the layers below, as depicted in Figure 1C. To evaluate the pH stability of the film we exposed the PEMs assembled on a QCM-D sensor to 500×10^{-3} M NaCl at different pHs, from pH 5 to pH 13. Films are assembled at pH 4.5, the pH at which complexes were formed. The initial pH to expose the multilayers was slightly acid and over 4.5, pH 5. We increased the pH in one unit until pH 13 (6, 7, 8, 9, etc.) exposing the film to a continuous flow for periods ranging from 5 to 12 h and then changing the flowing solution by a solution of higher pH. The frequency slightly decreases with variations of 0.2 Hz until pH 13, meaning that the film does not degrade in this range of pHs (Figure 3c). Frequency only increases at pH 13. The increase of the frequency is indicative of a partial degradation of the film. The stability experiments with QCM-D show that the multilayer is stable at physiological pH, 7.4, and suitable for biomedical applications.[48] Despite that the duration of the QCM-D measurements at pH 7, 12 h, is significantly shorter than the release experiments the multilayers were exposed at this pH long enough to cover the timeframe of the burst release without degrading. We can conclude that the release of gentamicin does not affect film stability.

Detailed SEM analysis PEM cross-section (**Figure 4**) revealed irregular topography with the highest areas measuring around 2 µm in height, correlating thus the high frequency changes monitored by QCM-D. The surface inhomogeneity was further confirmed by AFM analysis. **Figure 5** and Figure S4 (Supporting
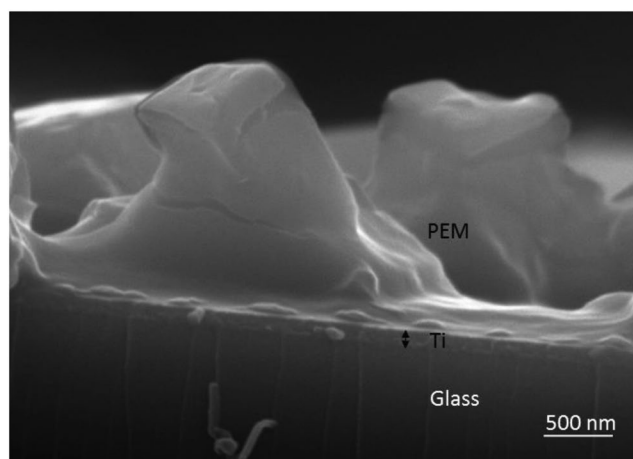
Figure 4. SEM cross-sectional image of the PEM deposited on top of the Ti film. The glass and the titania thin film can be distinguished, as well as the PEM grown on top of titania.

Information) show AFM images of height (a and d), phase (b) and height profile (c) of PEMs of PLL/PAA–gentamicin complexes. The roughness calculated from the height images of the PEM coating is 13.9 and 7.9 nm for the 15×15 µm (Figure 5a) and 5×5 µm (Figure S4a, Supporting Information) scans, respectively. The discrepancy in the roughness between the two images from the same sample confirms the data obtained from SEM (Figure 4), that the surface of the PEMs is rather inhomogeneous.[49] The inhomogeneity on the surfaces is probably the result of the large size dispersion shown by the complexes as observed by TEM and DLS. Phase images (Figure 5b; Figure S4b, Supporting Information) show that the lag in the phase remains constant over all scanned regions, suggesting that the LbL assembly is continuous without uncovered
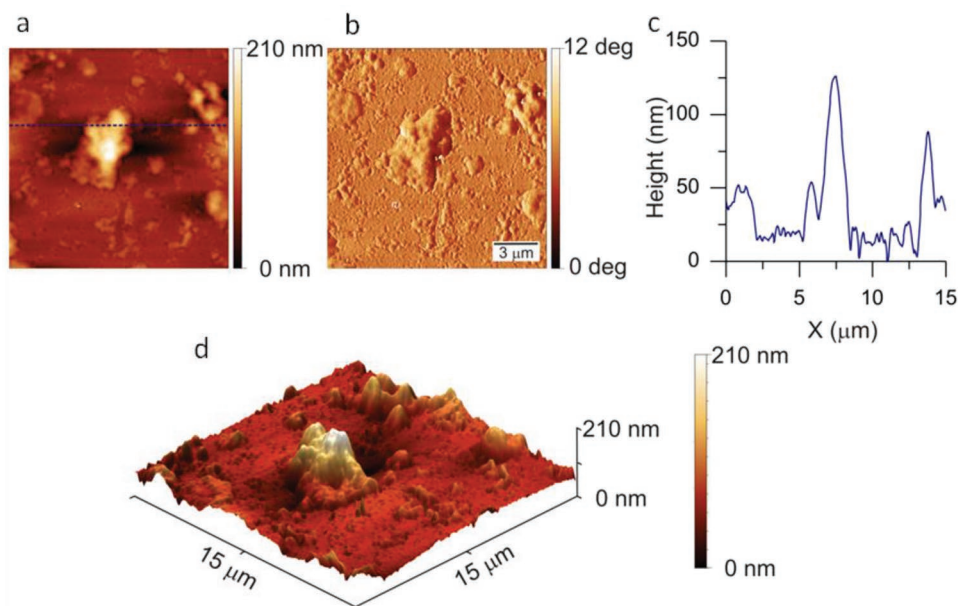
Figure 5. AFM images of the PEM of 4 PLL/PAA–gentamicin (0.3 mg mL^{-1}) complex bilayers. a) Height, b) phase, c) height profile of section at the dotted line in panel a, and d) 3D graph of the height of a 15 µm × 15 µm image.

1901373 (5 of 9)

regions. From the height profile we distinguish peaks of more than 100 nm, as well as regions with peaks of only a few nm and intermediate peaks with heights of around 50 nm can also be identified (Figure 5c; Figure S4c, Supporting Information). These images together with the QCM-D monitoring leads us to associate the exponential growth of the PLL-complex PEM to the island model. This model proposes that the first component is adsorbed in the surface forming "islands" and after several deposition steps the height and radius of the islands increases making the surface more and more heterogeneous and increasing the amount of material adsorbed.[50–52]

4. Gentamicin Release from PEMs

The advantage of encapsulating antibiotics close to the implant-tissue interface is the effective antibiotic release that leads to the side effects minimization.[53] Despite the PEMs being stable at physiological pH, we observed a release of gentamicin from the films. At physiological pH (7.4), gentamicin is less protonated than at pH 4.5, the pH at which the complexes were prepared. The deprotonation of gentamicin should weaken the interaction of the antibiotic with PAA, which should trigger gentamicin release. On the contrary, PAA has greater charge at higher pHs. We have seen that PAA and PLL multilayers fabricated with free PAA are stable at physiological pH. Since the stability of the film is largely due to the interaction of PLL with PAA, a stable film releasing gentamicin is possible. The total amount of gentamicin in the PEM is 5.35 µg. The amount of gentamicin released from the films can be monitored by measuring the fluorescence emission at 455 nm of the complex formed by gentamicin and the *O*-phthaldialdehyde (OPA) reagent. There is a burst release of gentamicin within the first 6 h, which liberates around 58% of the total gentamicin that is released during the whole experiment (inset in **Figure 6**). Then, after the burst
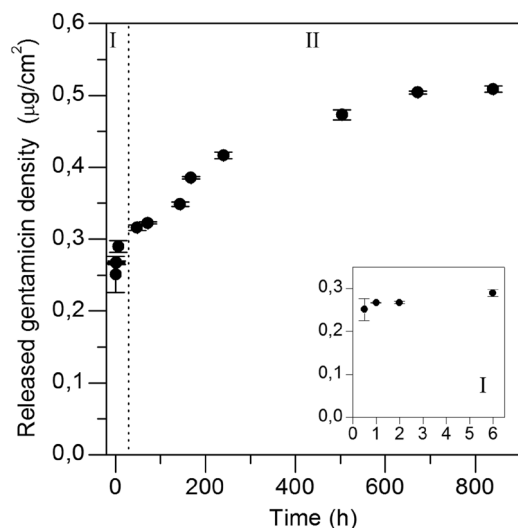
release, a prolonged release takes place. Gentamicin is slowly released in a period from 6 h to 35 d, after which a plateau is reached. This release profile of gentamicin encapsulated in the PEM has the characteristics required to avoid infections after a replacement surgery: (1) during the critical short-term postimplantation period, which lasts several hours, a burst release of gentamicin takes place. This burst release is needed to inhibit the initial adhesion of bacteria during the surgery, where there is the largest risk for infection as the body is opened and exposed. (2) A continued and slow release takes place beyond the initial first hours lasting weeks to avoid bacterial infection during the formation of a protective fibrous capsule and tissue integration on the implant.[54] The timeframe of the burst release at pH 7.4 is coincident with the QCM-D measurements at the same pH, which show that the film does not degrade. We can assume that the film remains stable over the whole release experiment; otherwise, we would measure a higher concentration of gentamicin in solution, which is not the case.

5. Evaluation of the Antibacterial Properties of the PEM

To demonstrate the antibacterial activity of the films, an *S. aureus* strain was seeded on top of the PLL/PAA–gentamicin PEMs. Samples were prepared under sterile conditions and glass immersed in gentamicin was used as a control. Approximately 1000 CFU of *S. aureus* were seeded at 37 °C for 24 h on three replicates for each sample. Transmission images show very few bacteria adhering to the surface of the film, while a larger number of bacteria are observed in the control (**Figure 7**a,b). This result suggests that the PEM has antibacterial properties. When bacteria were detached and incubated for 24 h on agar plates, the CFU for bacteria grown on control surfaces was four orders of magnitude higher than that for bacteria grown on the PEMs (Figure 7c).

6. Conclusion

Stable PAA–gentamicin complexes were synthesized by mixing 0.3 mg mL^{-1} gentamicin and 1 mg mL^{-1} PAA in 500×10^{-3} M NaCl at pH 4.5. Complexes display a hydrodynamic diameter ranging from 160 to 300 nm and are stable within 4 h. PEMs were constructed by alternating PLL and PAA–gentamicin complexes by adsorption on top of titania up to four bilayers. The assembly of the PAA–gentamicin complexes with PLL shows an exponential growth and a large number of PAA–gentamicin complexes are deposited with only a few assembled layers.

The PAA–gentamicin PEMs are stable until pH 13. However, PEMs release gentamicin at physiological pH. Release studies in phosphate buffered saline (PBS) buffer showed an initial burst release within the first 6 h followed by a slow release of gentamicin lasting up to five weeks. The antibacterial properties of the PEMs were tested by seeding an *S. aureus* strain on the LbL films. The CFU counts for bacteria grown on the PEMs after 24 h is four orders of magnitude smaller than those grown on a glass control immersed in gentamicin. It is important to

Figure 6. Release profile of gentamicin from PEMs formed of 4 bilayers of PLL/PAA–gentamicin complex on top of titania thin films. Region I shows the burst release (the insert is a zoom of region I) and region II the sustainable release. The release is followed up to 35 d using emission measurements at 455 nm.
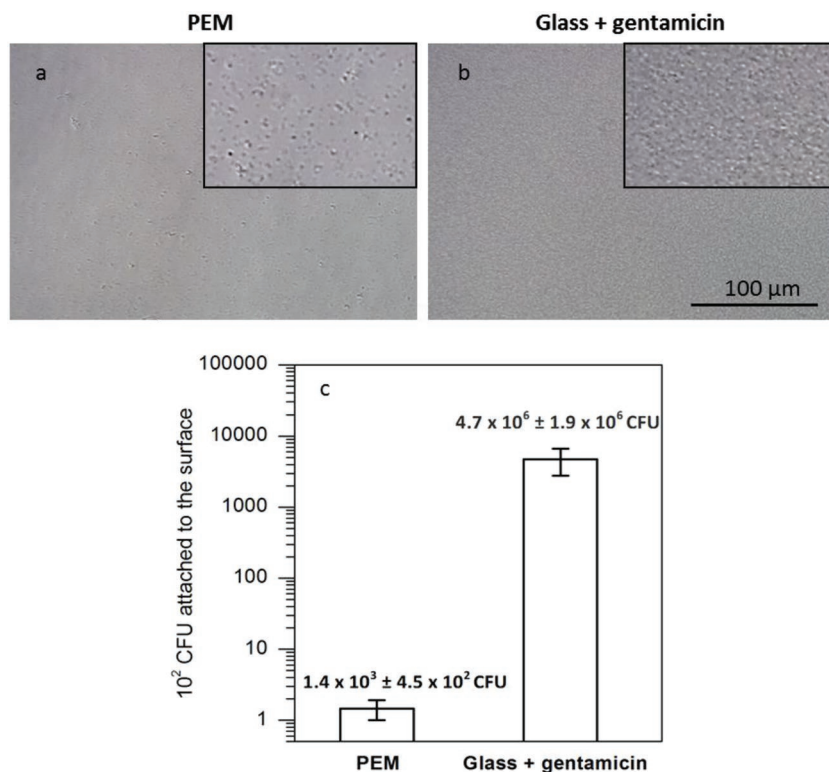
Figure 7. *S. aureus* growth on PAA–gentamicin PEM coatings and on glass substrates immersed in gentamicin. Cell observer images following 24 h of incubation of *S. aureus* on a) PEM coating on top of titania films and b) glass immersed in gentamicin, insert images are a zoom of 4×, c) CFU of the adhered bacteria on the PEM and glass with gentamicin.

note that only four bilayers of PLL and the complex are required to achieve a film with antibacterial properties.

During surgery and while the body is exposed to the environment, a fast release of gentamicin can be crucial for avoiding the attachment of bacteria. At the same time, a continuous supply of gentamicin in lower doses is required during the osseointegration process until the tissue is reconstituted to ensure that bacteria do not attach and proliferate at the site of the implant. The initial burst release of gentamicin followed by a long-lasting slow release over weeks makes the PAA–gentamicin PEMs especially attractive as an antibacterial coating for implants, and highlights the potential of these films to prevent nosocomial infections following implant surgery.

7. Experimental Section

Poly(acrylic acid) and Gentamicin Complexes: PAA and gentamicin complexes were prepared by mixing PAA and gentamicin at different ionic strengths: H_2O (0×10^{-3} M), 10×10^{-3} M, 500×10^{-3} M, and 2 M NaCl. Complexes were prepared with 1 mg mL^{-1} PAA ($M_w \approx 100$ kDa) and with 0.1, 0.25, 0.3, or 0.45 mg mL^{-1} gentamicin. The growth of the complexes was followed by measuring their size by DLS immediately after complex preparation, and at 2 and 4 h after preparation. Measurements were performed with a Zetasizer Nano ZS from Malvern. All measurements were repeated ten times. Complexes were visualized by TEM in a TEM JEOL JEM-1400PLUS microscope equipped with a Gatan US1000 CCD

camera. For TEM imaging, 5 µL of the complexes was deposited on a TEM grid (copper grids with a carbon film purchased from EM Resolutions), left to adsorb for 5 min, then rinsed three times with drops of distilled water. The sample was negatively stained by incubation for 5 min with 5 µL ammonium molybdate ((NH_4)$_2$MoO$_4$, Sigma Aldrich) at 20 ng mL^{-1} pH 6.7. Finally, the grid was rinsed three times with water drops.

Layer-by-Layer Assembly: PEMs were fabricated by means of the LbL technique on top of the titania films. A titania layer was deposited on top of glass discs through the sol–gel process. Briefly, titanium (IV) chloride (≥99.0%, TiCl$_4$ from Sigma Aldrich), ethanol absolute (Synthesis grade, EtOH from Scharlau), and nanopure water (H_2O) were mixed in a molar proportion of TiCl$_4$:EtOH:H_2O = 1:40:10. The titania precursor was prepared first, adding the TiCl$_4$ to the EtOH under vigorous stirring and left till drops to room temperature. Water was added and the sol was left stirring for 10 min to obtain a homogenous solution. 30 µL of the sol, previously mixed with EtOH in a volume proportion of sol:EtOH = 2:1, were spin coated at 68 rpm for 30 s on the glass coverslips of 14 mm in diameter and 0.13–0.16 mm of thickness from Thermo Scientific. Then, they were subjected to a thermal treatment: 30 min at 60 °C and another 30 min at 130 °C. Finally, they were calcinated; first, heating up with a ramp of 1 °C min^{-1} and then, keeping them at 350 °C for 2 h. For the LbL assembly the titania was first cleaned with absolute ethanol and dried at 100 °C. The PAA–gentamicin complexes and PLL solutions were prepared in 500×10^{-3} M NaCl at a pH of 4.5. A drop of 100 µL with PLL (1 mg mL^{-1}, $M_w \approx$ 150–300 kDa, Sigma Aldrich) was left incubating on titania for 15 min at room temperature, then to remove PLL in excess the surface was rinsed three times with 500×10^{-3} M NaCl pH 4.5 . Then, the same volume of PAA–gentamicin complex solution, prepared 2 h ago, was deposited on the surface left 15 min, removed and the surface was rinsed again three times as before. The alternating assembly of PLL and the complexes was repeated four times to obtain a multilayer of eight layers.

To measure the total amount of gentamicin, PEMs were disassembled in 1 mL 500×10^{-3} M NaCl at pH 13.

QCM-D Measurements: The assembly of PLL/PAA–gentamicin complexes multilayers was monitored via QCM-D with a Q-Sense E4 system. The LbL assembly was performed on QSX 303 SiO$_2$ quartz crystals. PLL and complexes were alternatively injected to the 4-sensor chamber with the help of a peristaltic pump and left to incubate for at least 10 min. For each deposition the solution was fluxed until frequency was stabilized, then a rinsing step of at least 10 min with 500×10^{-3} M NaCl solution at pH 4.5 took place. Experiments were conducted at 23 °C with a flux velocity of the solution of 100 µL min^{-1}. To study the stability of the multilayer under different pH conditions the multilayers were exposed in the QCM-D chamber to 500×10^{-3} M NaCl solutions with pHs ranging from 5 to 13. The solutions were fluxed at 5.77 µL min^{-1} and were changed once frequency reached a plateau.

SEM and AFM Imaging: A SEM of type JEOL JSM-6490LV was used. Samples were cut with a diamond tip and Pt–Au was sputtered in the preparation chamber GATAN ALTO1000. AFM images in dry state were acquired in air using a Nanowizard II AFM (JPK, Berlin, Germany). Images were acquired with tapping mode with the tip TESP-V2 (Bruker, AFM probes), which has a spring constant of 40 N m^{-1} and a resonant frequency in the range 280–320 kHz.

Gentamicin Release: Gentamicin release was studied by placing titania films coated with PEMs in a 24 multiwell dish. 1 mL of PBS was added

**ADVANCED
SCIENCE NEWS**

www.advancedsciencenews.com

**ADVANCED
MATERIALS
INTERFACES**

www.advmatinterfaces.de

to the wells with the sample. The release was measured at 30 min, 1, 2, and 6 h and 2, 3, 6, 7, 10, 21, 28, and 35 d. PBS solution was removed for each measurement from the well and replaced with fresh PBS. OPA reagent was prepared by mixing 0.2 g OPA dissolved in 1 mL methanol with 19 mL of 0.4 M boric buffer. The boric acid buffer was prepared by dissolving boric acid in distilled water and adjusting the pH to 10.4 with potassium hydroxide solution. Then, 0.4 mL of 2-mercaptoethanol was added and the pH adjusted to 10.4. This reagent was kept in the dark at 4 °C until use the following day. PBS solutions were removed from the well and then mixed with 2-propanol in a 1:1 ratio by volume and vortexed. Then, the OPA reagent was added in the same proportion and the solution was vortexed again.[55,56] Solutions were heated for 15 min at 60 °C to catalyze the reaction, prior to measurement. All reagents were purchased from Sigma Aldrich, except the 2-propanol, which was obtained from Fisher. Samples were prepared in triplicate and the average and standard error were calculated. The fluorescent complex was measured at 455 nm with a Thermo Scientific Varioskan Flash Multimode Reader. The calibration curve was performed for gentamicin concentrations ranging from 0 to 4 µg mL^{-1} containing seven points and was described with the following equation: $y = 6.49 + 21.26 \, x$ where y is the emission of the OPA-gentamicin complex at 455 nm and x is the gentamicin concentration in µg mL^{-1}; the coefficient of determination, R^2, is 0.997.

Antibacterial Test: The *S. aureus* strain RN4220 used here is resistant to erythromycin. It was cultured in Luria-Bertani (LB) broth from Lennox with 10 µL min^{-1} erythromycin (Sigma Aldrich) overnight at 37 °C under constant shaking at 200 rpm. For antibacterial tests, PEMs were assembled on titania under sterile conditions, immersed once in water and dried in air. They were placed in 24 multiwell dishes. For use as a control, round glass coverslips with a 14 mm diameter were immersed for 24 h in 0.3 mg mL^{-1} gentamicin in water and rinsed by immersing once in distilled water. Samples were prepared in triplicate. 1 mL of 1000 CFU mL^{-1} *S. aureus* in LB broth with 10 µL min^{-1} erythromycin was seeded in each well (containing the titania films with PEM coating or glass controls) and incubated for 24 h at 37 °C. After incubation, images were taken in transmission mode with a Cell Axio Observer Microscope. Samples were rinsed three times with PBS buffer to remove nonattached bacteria. Then, samples were vortexed for 1 min at 30 000 rpm in 10 mL PBS buffer to detach the bacteria. Dilutions were made in PBS. For titania films with the PEM coatings, the dilutions were 1/1 and 1/10, and for glass controls, were 1/1000 and 1/10 000. 100 µL of each dilution was placed in LB Agar (Lennox) sterile plates with 10 µg mL^{-1} erythromycin. In total, four plates of each sample were seeded; two at each dilution, and the colonies formed were counted following 24 h of incubation at 37 °C. Visual counting of the colony forming units (CFU) was performed and an average and standard error calculated.

Supporting Information

Supporting Information is available from the Wiley Online Library or from the author.

Conflict of Interest

The authors declare no conflict of interest.

[1] M. Cloutier, D. Mantovani, F. Rosei, *Trends Biotechnol.* **2015**, *33*, 637.

[2] W. F. Oliveira, P. M. S. Silva, R. C. S. Silva, G. M. M. Silva, G. Machado, L. C. B. B. Coelho, M. T. S. Correia, *J. Hosp. Infect.* **2018**, *98*, 111.

[3] F. D. Lowy, *N. Engl. J. Med.* **1998**, *339*, 520.

[4] D. Bhowmik, R. Bhanot, D. Gautam, P. Rai, K. P. S. Kumar, *Res. J. Sci. Technol.* **2018**, *10*, 165.

[5] W. M. Dunne, *Clin. Microbiol. Rev.* **2002**, *15*, 155.

[6] K. Lewis, *Antimicrob. Agents Chemother.* **2001**, *45*, 999.

[7] R. M. Donlan, J. W. Costerton, *Clin. Microbiol. Rev.* **2002**, *15*, 167.

[8] J. S. Moskowitz, M. R. Blaisse, R. E. Samuel, H.-P. Hsu, M. B. Harris, S. D. Martin, J. C. Lee, M. Spector, P. T. Hammond, *Biomaterials* **2010**, *31*, 6019.

[9] M. Butterworth, T. Payne, in *Complications in Foot and Ankle Surgery Management Strategies* (Eds: M. S. Lee, J. P. Grossman), Springer International Publishing, Cham **2017**, pp. 69–87.

[10] J. W. Costerton, P. S. Stewart, E. P. Greenberg, *Science* **1999**, *284*, 1318.

[11] E. S. McBryde, L. C. Bradley, M. Whitby, D. L. S. McElwain, *J. Hosp. Infect.* **2004**, *58*, 104.

[12] K. Rutledge-Taylor, A. Matlow, D. Gravel, J. Embree, N. Le Saux, L. Johnston, K. Suh, J. Embil, E. Henderson, M. John, V. Roth, A. Wong, J. Shurgold, G. Taylor, *Am. J. Infect. Control* **2012**, *40*, 491.

[13] R. M. Klevens, J. R. Edwards, C. L. Richards, T. C. Horan, R. P. Gaynes, D. A. Pollock, D. M. Cardo, *Public Health Rep.* **2007**, *122*, 160.

[14] T. Lin, E. Jämsen, L. Lu, K. Nathan, J. Pajarinen, S. B. Goodman, in *Orthopedic Biomaterials Progress in Biology, Manufacturing, and Industry Perspectives* (Eds: B. Li, T. Webster), Springer International Publishing, Cham **2018**, pp. 199–218.

[15] P. Stoica, M. C. Chifiriuc, M. Rapa, V. Lazăr, in *Biofilms and Implantable Medical Devices: Infection and Control* (Eds: Y. Deng, W. Lv), Elsevier inc., Amsterdam, Netherlands **2017**, pp. 3–23.

[16] I. Kurtz, J. Schiffman, I. S. Kurtz, J. D. Schiffman, *Materials* **2018**, *11*, 1059.

[17] A. Idrees, P. Varela, F. Ruini, J. M. Vasquez, J. Salber, U. Greiser, W. Wang, S. McMahon, S. Sartori, G. Ciardelli, V. Chiono, *Biomed. Sci. Eng.* **2018**, *2*, 39.

[18] M. R. E. Santos, P. V. Mendonça, M. C. Almeida, R. Branco, A. C. Serra, P. V. Morais, J. F. J. Coelho, *Biomacromolecules* **2019**, *20*, 1146.

[19] J. A. Lemire, J. J. Harrison, R. J. Turner, *Nat. Rev. Microbiol.* **2013**, *11*, 371.

[20] Q. Yu, Z. Wu, H. Chen, *Acta Biomater.* **2015**, *16*, 1.

[21] J. Gallo, M. Holinka, C. S. Moucha, *Int. J. Mol. Sci.* **2014**, *15*, 13849.

[22] B. Hu, C. Owh, P. L. Chee, W. R. Leow, X. Liu, Y.-L. Wu, P. Guo, X. J. Loh, X. Chen, *Chem. Soc. Rev.* **2018**, *47*, 6917.

[23] X. Ding, S. Duan, X. Ding, R. Liu, F.-J. Xu, *Adv. Funct. Mater.* **2018**, *28*, 1802140.

[24] A. Bassegoda, K. Ivanova, E. Ramon, T. Tzanov, *Appl. Microbiol. Biotechnol.* **2018**, *102*, 2075.

[25] S. Li, S. Dong, W. Xu, S. Tu, L. Yan, C. Zhao, J. Ding, X. Chen, *Adv. Sci.* **2018**, *5*, 1700527.

[26] G. Baier, A. Cavallaro, K. Friedemann, B. Müller, G. Glasser, K. Vasilev, K. Landfester, *Nanomed.: Nanotechnol., Biol. Med.* **2014**, *10*, 131.

[27] J. J. Richardson, M. Bjornmalm, F. Caruso, *Science* **2015**, *348*, aaa2491.

[28] N. J. Shah, M. L. Macdonald, Y. M. Beben, R. F. Padera, R. E. Samuel, P. T. Hammond, *Biomaterials* **2011**, *32*, 6183.

[29] J. Min, R. D. Braatz, P. T. Hammond, *Biomaterials* **2014**, *35*, 2507.

[30] M. L. Macdonald, R. E. Samuel, N. J. Shah, R. F. Padera, Y. M. Beben, P. T. Hammond, *Biomaterials* **2011**, *32*, 1446.

[31] D. Choi, M. Komeda, J. Heo, J. Hong, M. Matsusaki, M. Akashi, *ACS Biomater. Sci. Eng.* **2018**, *4*, 2614.

[32] S. Zhang, M. Xing, B. Li, S. Zhang, M. Xing, B. Li, *Int. J. Mol. Sci.* **2018**, *19*, 1641.

[33] S. B. Goodman, Z. Yao, M. Keeney, F. Yang, *Biomaterials* **2013**, *34*, 3174.

[34] G. Decher, *Science* **1997**, *277*, 1232.

[35] D. L. Elbert, A. Curtis, B. Herbert, J. A. Hubbell, *Langmuir* **1999**, *15*, 5355.

[36] E. Guzmán, A. Mateos-Maroto, M. Ruano, F. Ortega, R. G. Rubio, *Adv. Colloid Interface Sci.* **2017**, *249*, 290.

[37] M. Gürsoy, M. Karaman, in *In Surface Treatments for Biological, Chemical and Physical Applications* (Eds: M. Gürsoy, M. Karaman), Wiley **2017**, pp. 1–16.

[38] Q. An, T. Huang, F. Shi, *Chem. Soc. Rev.* **2018**, *47*, 5061.

[39] M. L. Cortez, A. Lorenzo, W. A. Marmisollé, C. von Bilderling, E. Maza, L. Pietrasanta, F. Battaglini, M. Ceolín, O. Azzaroni, *Soft Matter* **2018**, *14*, 1939.

[40] G. Romero, O. Ochoteco, D. J. Sanz, I. Estrela-Lopis, E. Donath, S. E. Moya, *Macromol. Biosci.* **2013**, *13*, 903.

[41] A. Díez-Pascual, P. Shuttleworth, *Materials* **2014**, *7*, 7472.

[42] P. Baudoux, N. Bles, S. Lemaire, M.-P. Mingeot-Leclercq, P. M. Tulkens, F. Van Bambeke, *J. Antimicrob. Chemother.* **2006**, *59*, 246.

[43] C. J. Tainter, Y. Ni, L. Shi, J. L. Skinner, *J. Phys. Chem. Lett.* **2013**, *4*, 12.

[44] M. C. Dixon, *J. Biomol. Tech.* **2008**, *19*, 151.

[45] L. Séon, P. Lavalle, P. Schaaf, F. Boulmedais, *Langmuir* **2015**, *31*, 12856.

[46] L. Peng, F. Cheng, Y. Zheng, Z. Shi, W. He, *Langmuir* **2018**, *34*, 10748.

[47] C. Su, J. Sun, X. Zhang, D. Shen, S. Yang, C. Su, J. Sun, X. Zhang, D. Shen, S. Yang, *Polymers* **2017**, *9*, 114.

[48] J. M. Anderson, A. Rodriguez, D. T. Chang, *Semin. Immunol.* **2008**, *20*, 86.

[49] A. Bonyár, *Micron* **2016**, *87*, 1.

[50] D. T. Haynie, E. Cho, P. Waduge, *Langmuir* **2011**, *27*, 5700.

[51] V. I. Kulikouskaya, M. E. Lazouskaya, A. N. Kraskouski, V. E. Agabekov, *Russ. J. Phys. Chem. A* **2018**, *92*, 146.

[52] V. I. Kulikouskaya, S. V. Pinchuk, K. S. Hileuskaya, A. N. Kraskouski, I. B. Vasilevich, K. A. Matievski, V. E. Agabekov, I. D. Volotovski, *J. Biomed. Mater. Res., Part A* **2018**, *106*, 2093.

[53] M. Arruebo, N. Vilaboa, J. Santamaria, *Expert Opin. Drug Delivery* **2010**, *7*, 589.

[54] J. M. Anderson, *Annu. Rev. Mater. Res.* **2001**, *31*, 81.

[55] J. Krzek, H. Woltyńska, U. Hubicka, *Anal. Lett.* **2009**, *42*, 473.

[56] J. Gubernator, Z. Drulis-Kawa, A. Kozubek, *Int. J. Pharm.* **2006**, *327*, 104.